Improvement of precision in spatial localization of radio-opaque markers using the two-film technique

Kwok L. Lam and Randall K. Ten Haken
Department of Radiation Oncology, University of Michigan, Ann Arbor, Michigan 48109-0010

(Received 28 November 1990; accepted for publication 25 March 1991)

Radio-opaque markers implanted inside or placed on the skin of patients can be used to detect set-up errors and patient motion. The effects of imaging geometry accuracy for standard radiotherapy equipment on the precision of calculating the positions of radio-opaque spherical markers using two orthogonal radiographic film projections is investigated. Inaccuracies in the imaging geometry are computed from the manually digitized positions of the marker images on each film pair. Actual marker locations are calculated with a precision limited only by the variance in manual digitization by incorporating those imaging geometry inaccuracies into their computation. Results of a phantom study using a grid of markers in a plastic block indicate that submillimeter precision can be obtained for the spatial coordinates of individual markers, and that the precision is not sensitive to the small inaccuracies in imaging geometry present within the mechanical tolerances of modern radiotherapy treatment machines and simulators.

I. INTRODUCTION

Spatial localization of points from images on orthogonal films is a process with many applications in radiation oncology. In brachytherapy, the locations of radioactive sources are reconstructed using two or three projections on radiographs.[1] Locating the positions of radio-opaque markers affixed to the patient on film pairs can also be used to help determine patient external anatomy,[2] or as an aid in registering imaging studies with simulator and port films.[3,4] Similarly, radio-opaque markers placed on or implanted in patients can be used for the determination of the position and orientation of the patient relative to the treatment machine, which has led to recent proposals for their use in automated patient set-up for conformal therapy[5] and fractionated stereotactic radiosurgery.[6]

Usually the three-dimensional coordinates of the points are determined based on the assumption that the imaging geometry is accurate and that there is no patient motion between the different projections. As the error due to patient motion between projections can be eliminated by simultaneously acquiring the different projections, the studies below were limited to the assessment of the error due to the finite tolerance in the accuracy of the equipment. Linear-algebraic methods have been developed previously to determine the imaging geometry and three-dimensional structure from two projections[7,8] in computer vision and biplane radiography. An extension of the method using least-square estimate for an overdetermined problem has also been published.[9] However, these methods require at least eight markers to cast the problem into a form solvable by linear-algebraic techniques and they do not allow solutions for selected subsets of the imaging geometry parameters (equivalent in radiotherapy to gantry angles, collimator angles, etc. of the two projections).

In this study, the random error in manual digitization of the marker images is determined for a standard system and a method is developed to reduce the uncertainty in 3-D localization of points to a level limited by that random error. The inaccuracies of the imaging geometry are estimated by a multidimensional nonlinear optimization algorithm using information on the radiographs. The inaccuracies are then incorporated into the calculation of the coordinates. Finally, the effect of the precision of manual digitization and the inaccuracies in imaging geometry on the precision and accuracy of the estimated coordinates of spherical radio-opaque markers has been evaluated.

II. MATERIALS AND METHODS

A phantom consisting of 25 markers embedded at machined locations in a plastic block was constructed to study the precision of spatial localization of markers. The markers (1.58-mm-diam tungsten carbide ball bearings[10]) were placed in the phantom at 1-cm spacing on a 4×4-cm rectangular grid. Orthogonal films were taken on a radiation therapy treatment simulator[11] and with the 6-MV beam of a linear accelerator.[12]

For the simulator films, the phantom was placed on the patient table at isocenter with the grid pattern rotated $\sim 11°$ about the vertical axis. With the x-ray tube (gantry) rotated 11° down from vertical, three exposures on the same film were obtained by moving the table vertically up by 1.000 cm between each exposure. The gantry was then moved by 90° to 11° above horizontal, orthogonal to the previous location. Three exposures were then taken on another film with the table lowered by 1.000 cm between each exposure. All vertical displacements were measured by a dial indicator to a precision of 0.002 cm. Magnification of the isocenter grid at the film was 1.58. The result was a pair of films with orthogonal projections of 75 markers such that sets of 25 markers were equally spaced one centimeter apart in the vertical direction. The two 11° offsets were employed to prevent the images of the markers from overlapping each other on the films. The locations of the marker images on the films were

 0094-2405/91/061126-06$01.20

digitized into a computer using a light box tablet and an electromagnetic digitizer.[13] The digitizer tablet has a puck with a crosshair that is centered over each point to be digitized. The coordinate system on the films was defined by the image of the thin radio-opaque wires stretched across the collimator of the simulator (simulator crosshair).

The linear accelerator did not have a film cassette holder attached to the gantry. To maintain high accuracy in positioning the film cassette, the orthogonal films were taken with the gantry in the vertical and the horizontal direction instead of 11° from vertical and horizontal. The plane of the phantom containing the markers was rotated approximately 45° about the gantry axis to prevent images of the markers from overlapping each other on the films. The focal-spot-to-film distances were 125.4 cm for the vertical projection and 133.4 cm for the horizontal projection. Four orthogonal pairs of localization films were taken: with the phantom at isocenter, 1.34 cm above isocenter, 2.64 cm above isocenter and 3.97 cm above isocenter, respectively. The height of the phantom was changed by placing plastic spacers under it and its orientation was checked after each change using the patient laser alignment system in the treatment room. The images of the markers and the corners of the x-ray field were digitized for each of the four sets of films. The coordinate system was defined by the center of the fields with axes parallel to the edges of the fields. The market images from the four film pairs were combined to simulate the images that would have been obtained from a phantom with layers of 25 markers separated by 1.34, 2.64, and 3.97 cm from the bottom layer, respectively.

A film taken with the x-ray tube 11° from vertical on the simulator and a film taken with the gantry horizontal on the linear accelerator were both taken through the complete digitization process twice to study the precision of manual digitization (i.e., after initial digitization, each film was remounted at a different location on the digitizer tablet). The vector differences between the coordinates of the marker images for the two digitizations were calculated. The distances between those difference vectors and their centroid were computed. The root mean square (rms) of those distances was taken to be the error in manual digitization D. If $\mathbf{u}_i'$ is the coordinate of the image of marker i in the first digitization and $\mathbf{u}_i$ is that in the second digitization, then

$$D = \sqrt{N^{-1}\sum_i |(\mathbf{u}_i' - \mathbf{u}_i) - N^{-1}\sum_j (\mathbf{u}_j' - \mathbf{u}_j)|^2}. \quad (1)$$

The line that was perpendicular to and intersecting the two rays joining the x-ray focal spots to the marker image on the films for the two projections (Fig. 1) was determined to obtain the three-dimensional locations of a marker from each film pair. The location of the marker was taken to be the midpoint of the intersections and the separation between the two intersections was the minimum separation between the two rays for the particular marker. The squares of the minimum separations were averaged over all the markers and the observed rms minimum separation S_0 was defined as the square root of that average.

The expected rms minimum separation limited by manual digitization alone S_e was estimated as follows. Assuming

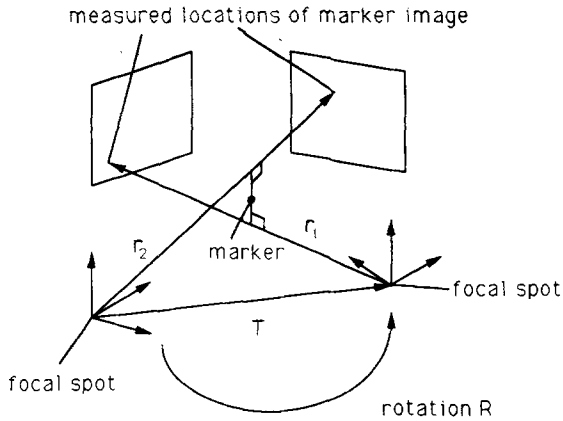

FIG. 1. Geometry for the reconstruction of a marker position. T is the translation vector between the two focal spot locations and R is the rotation matrix between the two coordinate systems with origins at the two focal spots, respectively.

that the error in manual digitization was isotropic, and that the errors in any two orthogonal directions on the film were uncorrelated, then the variance of the location of the marker images projected on the film in the direction of the minimum separation vector would have been half the square of the error in manual digitization D (errors in manual digitization perpendicular to direction of minimum separation vector have negligible contribution to S_e). Letting θ represent the angle between the direction of minimum separation projected on the film and the direction of minimum separation, the mean of the squares of minimum separation due to the uncertainty in manual digitization of this film would have been

$$\tfrac{1}{2}(D\cos\theta/M)^2, \quad (2)$$

where M is the magnification of the projection. If the uncertainty in the error of manual digitization were uncorrelated for the two films, then

$$S_e = \frac{D}{\sqrt{2}}\sqrt{\left(\frac{\cos\theta_1}{M_1}\right)^2 + \left(\frac{\cos\theta_2}{M_2}\right)^2}, \quad (3)$$

where subscripts 1 and 2 denoted corresponding values for the two projections. For markers near the isocenter, θ_1 and θ_2 could be taken as zero.

Following Metz and Fencil,[8] we characterized the relationship between the two projections by the translation vector T of the displacement of the focal spot and the rotation matrix R of the rotation of the collimator coordinate system (Fig. 1). The collimator coordinate system rotates as the collimator and the gantry rotate. T and R could be calculated from the imaging geometry (gantry angles, collimator angles, etc.) indicated by the equipment. If the imaging geometry indicated by the equipment was accurate, T and R would be accurate and the observed rms separation S_0 would be equal to the expected rms separation S_e. If the imaging geometry was allowed to be inaccurate, then T and R would be inaccurate and S_0 would be larger than S_e in general. This would imply that elements of the rotation matrix R, and the vector T were parameters that could be adjusted to minimize S_0. A multidimensional minimization algorithm[14] was used

to search for the minimum using the **T** and R calculated from the imaging geometry as indicated by the equipment as an initial guess. This local search method was judged to be more appropriate for the problem at hand than algebraic methods because only small inaccuracies in imaging geometry were to be solved and the parameters to be adjusted could be selected. As there were four coordinates from the two films for each marker, and for each marker only the three spatial coordinates in 3-D space were determined, each marker provided an extra degree of freedom for determination of R and **T**[8]. As the number of markers was more than the number of parameters, the extra information was used to reduce error.

To evaluate the relative importance of the parameters, minimizations were performed using different combinations of the parameters. There are three degrees of freedom for the rotation matrix R and three degrees of freedom for the translation vector **T**. However, the same marker image coordinates can be obtained for different magnitudes of **T**[8]. So only two degrees of freedom corresponding to the orientation of **T** could be recovered. The total number of degrees of freedom for the problem was then five. The five parameters chosen were the polar and azimuthal angle of **T** with respect to the coordinate system of the first projection, the orientation of the central axis of the second projection with respect to the first projection, and the rotation of the coordinate system about that central axis. The central axis was defined as the ray from the source to the intersection of the crosshair image for the simulator and from the source to the center of the x-ray field for the linear accelerator.

The polar angle of **T** was 90° minus half of the gantry rotation between projections and the gantry angle was used as one minimization search parameter. The orientation of the central axis defined two more search parameters as the coordinates of the intersection of the central axis with the film plane, which was effectively the shift of the crosshair image for the simulator (the shift of the center of field for the linear accelerator). The azimuthal angle of **T** was the collimator angle of the first projection. The rotation of the coordinate system about the central axis was the collimator angle of the second projection. For the last two parameters, the collimator angles of the two projections were replaced, for convenience, by the average collimator angle and the difference in collimator angle of the two projections.

To evaluate the effect of the inaccuracies in imaging geometry on the estimated coordinate of the markers, we expressed the estimated three-dimensional coordinates of a marker with inaccuracies x_i' as a function of the three-dimensional coordinates of the marker with accurate imaging geometry x_i and the parameters characterizing the imaging geometry inaccuracies (such as gantry angles, etc.) p_j:

$$x_i' = f_i(x_1, x_2, x_3, p_1, \ldots, p_n), \tag{4}$$

where $i = 1,2,3$ corresponding to the three coordinates, and n is the number of parameters. The expression can be expanded by Taylor's expansion about $x_i = 0$ and p_j's corresponding to accurate imaging geometry. Terms up to first order in x_i's are kept. This gives

$$x_i' = x_i + \sum_j \left(\frac{\partial f_i}{\partial p_j}\right)\Delta p_j + \frac{1}{2}\sum_{j,k}\left(\frac{\partial^2 f_i}{\partial p_k\, \partial x_j}\right)\Delta p_k x_j. \tag{5}$$

The error $(x_i' - x_i)$ is then given by

$$(x_i' - x_i) = a_i + \sum_j b_{ij} x_j, \tag{6}$$

where

$$a_i = \sum_j \left(\frac{\partial f_i}{\partial p_j}\right)\Delta p_j$$

and

$$b_{ij} = \frac{1}{2}\sum_k \left(\frac{\partial^2 f_i}{\partial p_k\, \partial x_j}\right)\Delta p_k.$$

The coefficients a_i and b_{ij} were computed numerically. It can be seen from Eq. (6) that both a_i and b_{ij} affect the accuracy in determining the coordinates of markers but only b_{ij} affects the accuracy in determining the difference in coordinates between two markers or the displacement of a marker. In the study, the phantom was displaced by known amounts. The displacement vectors were determined both with and without imaging geometry correction, and the differences were compared with the numerical result of Eq. (6) by assuming that the corrected imaging geometry was the accurate geometry.

III. RESULTS

A. Precision of manual digitization

The differences in coordinate of the marker images for the two manual redigitizations of a simulator film and a linear accelerator film were plotted as scatter plots (Fig. 2). The centroid of the data pints for the simulator film [Fig. 2(a)] has a systematic shift of -0.002 cm in x and -0.012 cm in y. That shift between the two digitizations is interpreted as being due to the error in digitizing the location of the simulator crosshair image. The rms distance D between the data points and their centroid is 0.009 cm. For the images on the localization films from the linear accelerator [Fig. 2(b)], D increases to 0.023 cm.

B. Evaluation of the rms minimum separation

The observed rms minimum separation between the rays generated from the 75 marker images taken from the film pairs S_0 on the simulator is 0.079 cm. The corresponding S_0 for the 100 marker images taken on the linear accelerator is 0.041 cm. The expected rms minimum separation from error in manual digitization S_e [Eq. (3)], for the simulation films was 0.007 cm and that for the localization films was 0.018 cm. The expected and observed rms minimum separations from the simulation films and the localization films do not agree. The increases in S_0 over S_e are interpreted as being due to the deviation of the imaging geometry from what was indicated on the equipment.

C. Correction for imaging geometry inaccuracies

The S_0's could be reduced by allowing for inaccuracies in the imaging geometry. Out of the selected parameters for minimization of the S_0's (gantry rotation between the two projections, average and difference of collimator angle between the two projections, and crosshair shift of the second

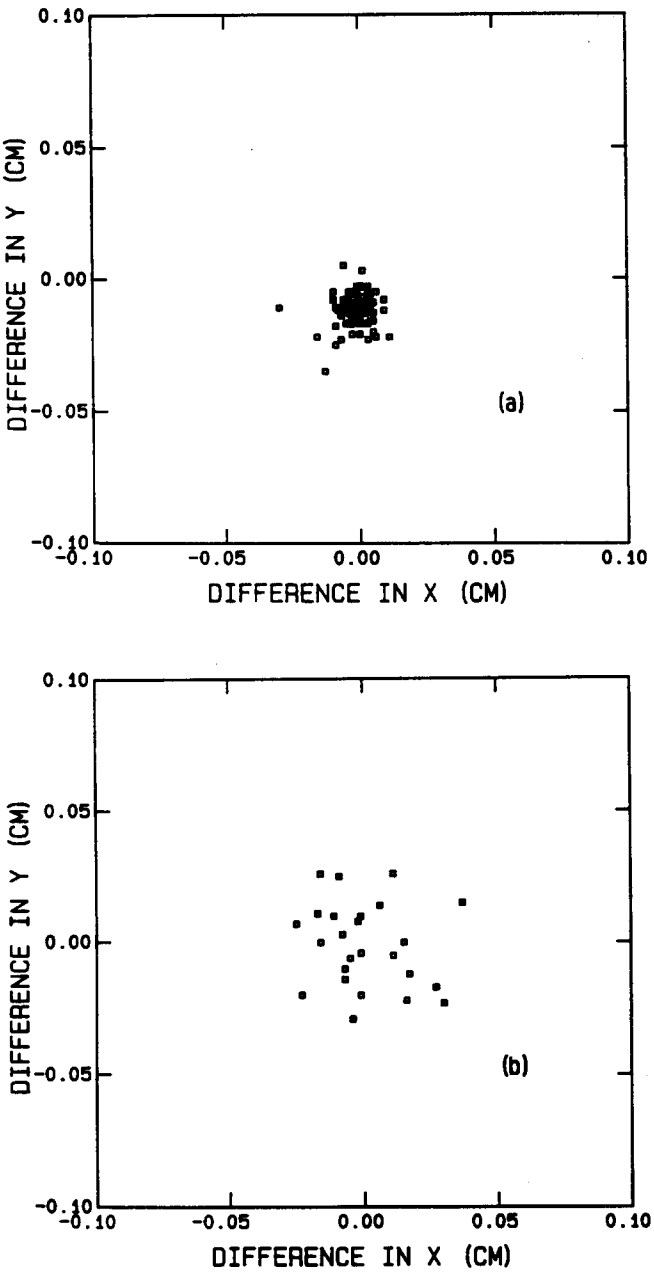

FIG. 2. Variation of the coordinates of marker images on an x-ray film from two digitizations of the same film. (a) Result for the 75 marker images on simulation film. (b) Result for the 25 marker images on localization film.

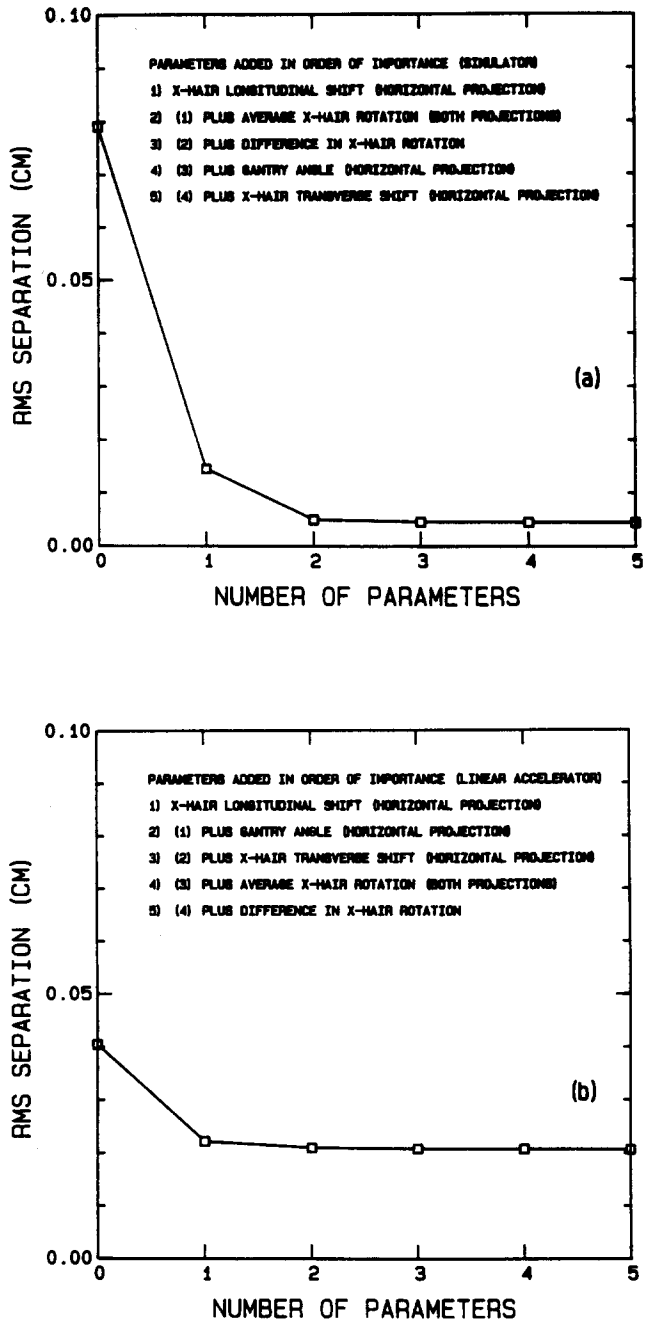

FIG. 3. Dependence of the rms minimum separation averaged over all markers, on the number of parameters allowed in the minimization algorithm. (a) Data taken on the simulator. Number of parameters are accumulatively included according to the order of importance. (b) Data taken on the linear accelerator. Only the x-ray field longitudinal shift on the lateral film and x-ray field transverse shift on both films were important in the algorithm.

projection), the most important one for our simulator is crosshair longitudinal shift, with correction for the average collimator angle next in importance [Fig. 3(a)]. The introduction of a third parameter leads to an insignificant improvement. The crosshair longitudinal shift is 0.125 cm at the film plane, corresponding to 0.08 cm at isocenter. The correction for the collimator angle is 0.5 deg. The S_0 after correction for the parameters, 0.004 cm [baseline value in Fig. 3(a)], is comparable to what would be expected if variation in manual digitization was the only source of error.

For the liner accelerator, the longitudinal shift of the center of the field (equivalent to crosshair shift for simulator) is also the most important parameter, but the rest of the parameters give insignificant reduction in S_0 [Fig. 3(b)]. The longitudinal shift is 0.045 cm at the film plane, which is 0.034 cm at isocenter. As above, corrections for imaging geometry inaccuracies also improves S_0 to 0.021 cm, a value comparable to that due to manual digitization alone.

It was also found that after S_0 had been reduced to the level of manual digitization error, adding more parameters

to the minimization algorithm sometimes gave unreasonable results for the parameters. For example, introducing crosshair transverse shift together with the longitudinal shift minimized S_0 for a transverse shift of 0.675 cm and a longitudinal shift of 0.045 cm (both at film plane). The x-ray field did not have a 0.675 cm transverse shift with respect to the isocenter. The minimization algorithm was trying to minimize the random error from manual digitization by adjusting the crosshair transverse shift, giving an unreasonable result for this parameter. So, it is important to be able to select parameters in the estimation of the inaccuracies in imaging geometry. Only parameters that reduced S_0 significantly were used to obtain estimated coordinates of the markers.

D. Accuracy and precision of the locations of markers

Since the 25 markers of the grid phantom were moved by 1.000 cm between exposures on the simulator, the displacement vectors from each marker of the original set to the corresponding marker of the displaced set was expected to be 0.000 cm in x, -1.000 cm in y, and 0.000 cm in z. The average displacement actually determined for the 25 markers was -0.003 cm in x, -0.998 cm in y, and 0.001 cm in z. The variation of displacement vectors among the 25 markers can be characterized by a rms distance of 0.009 cm from the average displacement vector. When inaccuracies of imaging geometry were not incorporated, the result was the same except for the z displacement, which is -0.003 cm instead of 0.001 cm, i.e., a difference of 0.004 cm. The result for a 2.000 cm displacement was similar, with an average displacement of -0.003 cm in x, -1.993 cm in y, and 0.002 cm in z and a rms distance of 0.007 cm from the average displacement. Without imaging geometry correction, the only difference was that the z displacement was -0.006 cm instead of 0.002 cm (0.008-cm difference).

For the linear accelerator, the results for the y displacements of -1.34 cm, -2.64 cm, and -3.97 cm were: average displacements of $(-0.038, -1.31, -0.027)$, $(-0.028, -2.61, 0.003)$, and $(-0.050, -3.95, 0.007)$, and rms distances of 0.021, 0.024, and 0.025 cm, respectively. The results without imaging geometry correction were the same.

Numerical results of a and b in Eq. (6) for one mm of crosshair longitudinal shift at isocenter are

$$a = \begin{pmatrix} 0.0\text{ mm} \\ 0.0\text{ mm} \\ 0.5\text{ mm} \end{pmatrix}, \quad b = \begin{pmatrix} 0.0000 & 0.0000 & 0.0005 \\ 0.0000 & 0.0000 & 0.0005 \\ -0.0005 & 0.0000 & 0.0000 \end{pmatrix}.$$

The results for 1 degree of average collimator rotation are

$$a = \begin{pmatrix} 0.0\text{ mm} \\ 0.0\text{ mm} \\ 0.0\text{ mm} \end{pmatrix}, \quad b = \begin{pmatrix} 0.0000 & 0.0000 & -0.0174 \\ 0.0000 & 0.0000 & -0.0174 \\ 0.0087 & 0.0087 & 0.0000 \end{pmatrix}.$$

For the simulator, the imaging geometry correction was 0.8-mm longitudinal shift and 0.5-deg collimator rotation. Since a and b are proportional to the parameters of the inaccuracy in imaging geometry [Eq. (6)], a and b for the simulator are

$$a = \begin{pmatrix} 0.0\text{ mm} \\ 0.0\text{ mm} \\ 0.4\text{ mm} \end{pmatrix}, \quad b = \begin{pmatrix} 0.0000 & 0.0000 & -0.0083 \\ 0.0000 & 0.0000 & -0.0083 \\ 0.0040 & 0.0044 & 0.0000 \end{pmatrix}.$$

This predicts a difference of 0.0044 cm per cm of displacement in the y direction (second column in b). It compares well the 0.004-cm difference observed for the 1-cm displacement and 0.008-cm difference for the 2-cm displacement. For the linear accelerator, the imaging geometry correction was 0.034 cm of crosshair longitudinal shift. Since elements in the second column of b for crosshair longitudinal shift are zero's, no difference in displacement vectors is expected and it is confirmed by the experimental results.

IV. DISCUSSION

The results show that manual digitization of circular marker images on film can be performed with good repeatability ($\sim$0.01 cm on simulator films and $\sim$0.02 cm on localization films). The center of the image can be accurately determined visually by dividing the circle into four equal sectors using the crosshair on the puck of our digitizer system. This degree of precision should not be generalized to images of other shapes. The degradation in precision for the localization film relative to the simulation film is probably due to the fuzzier edges and the lower contrast of the marker images seen on that film.

By incorporating inaccuracies in imaging geometry deduced from the images on the films, the minimum rms separation of marker coordinates from the two film projections could be reduced to that limited by manual digitization alone and the coordinates of an individual marker could be determined to submillimeter precision. In the present case, only the crosshair longitudinal shift on the horizontal projection had a significant impact on precision and all other parameters had minimal or no effect on rms separation. Although in both cases incorporation of the inaccuracy of imaging geometry into the computation reduced rms separations to the level due to manual digitization alone, the magnitude of the overall changes in the coordinates themselves were not great. Changes of 0.04 cm in addition to an increase of less than 0.01-cm change per cm of estimated coordinate of the markers were introduced on the simulator. The corresponding changes for the films taken on the linear accelerator was 0.017 cm in addition to less than 0.0002 cm per cm.

From the results above, it could be concluded that for use of similar equipment for the determination of marker coordinates from film pairs (taken, for example, from a linear accelerator with good mechanical integrity) with respect to a given coordinate system (established, for example, on a simulator), inaccuracies in imaging geometry need to be corrected only if error less than 0.05 cm is required. When relative vectors on the same machine are sought, only b is important and the error is less than 0.01 cm per cm in the difference vector. This is the case when the technique is employed for the detection of day to day patient set-up error and brachytherapy source localization. Therefore, clinically significant errors in the determination of marker movement (e.g., 0.05 cm) on the same machine would only be found for large ($\sim$5 cm) values of the difference vector. As set-up errors are

usually less than a few centimeters, the correction for inaccuracies in imaging geometry is probably not necessary.

Although the experiments were done with orthogonal projections, the methods do not require the projections to be orthogonal. Both the correction of imaging geometry and the estimation of errors due to inaccuracies in imaging geometry can be applied to two-film technique in general. Further investigations are required to evaluate the performance of the two-film technique between the two limiting cases of orthogonal projections and stereo projections.

ACKNOWLEDGMENT

We would like to thank Steve Hardybala for the construction of the phantom.

[1]R. L. Siddon and L. M. Chin, "Two-film brachytherapy reconstruction algorithm," Med. Phys. **12**, 77–83 (1985).

[2]D. A. Christopherson and D. Jones, "A general approach to the location of radiopaque objects, with applications in radiotherapy," Phys. Med. Biol. **29**, 1581–1586 (1984).

[3]D. R. Haynor, A. W. Borning, B. A. Griffin, J. P. Jacky, I. J. Kalet, and W. P. Shuman, "Radiotherapy planning: Direct tumor location on simulation and port films using CT," Radiology **158**, 537–540 (1986).

[4]B. A. Fraass, D. L. McShan, R. F. Diaz, R. K. Ten Haken, A. Aisen, S. Gebarski, G. Glazer, and A. S. Lichter, "Integration of magnetic resonance imaging into radiation therapy treatment planning: I. Technical considerations," Int. J. Radiat. Oncol. Biol. Phys. **13**, 1897–1908 (1987).

[5]R. K. Ten Haken, D. L. McShan, A. Gerhardsson, A. F. Thornton, Jr., and B. A. Fraass, "Use of radio-opaque markers in automated patient set-up," Med. Phys. **16**, 678 (1989) (Abstract).

[6]D. Jones, D. Christopherson, M. D. Hafermann, J. Rieke, J. Travaglini, and S. Vermeulen, "Experience with a technique for fractionated radiosurgery," Int. J. Radiat. Oncol. Biol. Phys. **19** (Supplement 1), 134 (1990) (Abstract).

[7]H. C. Longuet-Higgins, "A computer algorithm for reconstructing a scene from two projections," Nature **293**, 133–135 (1981).

[8]C. E. Metz and L. E. Fencil, "Determination of three-dimensional structure in biplane radiography without prior knowledge of the relationship between the two views: Theory," Med. Phys. **16**, 45–51 (1989).

[9]J. Weng, T. S. Huang, and N. Ahuja, "Motion and structure from two perspective views: algorithms, error analysis, and error estimation." IEEE Trans. Pattern Anal. Machine Intell. **11**, 451–476 (1989).

[10]Industrial Tectonics, Inc., Ball Division, Dexter, Michigan.

[11]Simulix-Y, Oldeft Corporation of America, Fairfax, Virginia.

[12]Clinac 1800, Varian Associated, Inc., Palo Alto, California.

[13]ACT 23-2 BL, Altek Corporation, Silver Spring, Maryland.

[14]W. H. Press, B. P. Flannery, S. A. Teukolsky, and W. T. Vetterling, *Numerical Recipes* (Cambridge U. P., New York, 1986), pp. 289–293.